ARTICLE

Thermographic Observation of High-Frequency Ethanol Droplet Train Impingement on Heated Aluminum and Glass Surfaces

Baris Burak Kanbur, Sheng Quan Heng and Fei Duan[*]

School of Mechanical and Aerospace Engineering, Nanyang Technological University, 639798, Singapore
[*]Corresponding Author: Fei Duan. Email: feiduan@ntu.edu.sg

ABSTRACT

The present study considers the impingement of a train of ethanol droplets on heated aluminum and glass surfaces. The surface temperature is allowed to vary in the interval 140°C–240°C. Impingement is considered with an inclination of 63 degrees. The droplet diameter is 0.2 mm in both aluminum and glass surface experiments. Thermal gradients are observed with a thermographic camera. It is found that in comparison to glass, the aluminum surface displays very small liquid accumulations and better evaporation performance due to its higher thermal conductivity. The relatively low thermal conductivity of glass results in higher thermal gradients on the surface. The droplet impact area on the aluminum surface is smaller than the corresponding area for the glass surface. Interestingly, the liquid accumulation area is not symmetrical. Moreover, the extension of the droplet train impact region decreases on increasing the surface temperature because higher temperature values allow greater surface energy levels that enhance significantly the evaporation rate.

Nomenclature

d	Droplet diameter in air, mm
D	Droplet nozzle, μm
f	Frequency, kHz
l	Spacing between adjacent droplets, mm
T	Temperature, °C
Re	Reynolds number
w	Surface wall
We	Weber number
ν	Droplet velocity, m/s
μ	Viscosity, Pa·s
ρ	Density, kg/m^3
σ	Surface tension, N/m

1 Introduction

Droplet impingement studies provide a broad understanding of boiling behaviors and evaporation trends of liquids on target surfaces in various engineering applications like drop-on-demand additive manufacturing, inkjet printing, spray cooling, and thermal management of electronics [1–3]. The single droplet impingement approach is the traditional and well-known type of droplet impingement studies. Thanks to the single droplet impingement, physical understanding of droplet wetting area, oscillation, rebounding, etc. can be understood. Thereby, hydrodynamics- or heat transfer-related improvements can be pointed out [4]. However, it is known that real applications are conducted with multiple droplet impingements that makes the boiling and evaporation trends more complex. In a multiple and continuous droplet impingement process, additional physical phenomena like splashed droplets, splashing directions, crown formation, spreading length become crucial but they cannot be investigated with a single droplet impingement study. Hence, another droplet impingement technique, which is called the droplet train impingement method, is applied on the target surfaces. Droplet train impingement studies are more complex to investigate but they can mimic the droplet-droplet and droplet-surface interactions of advanced engineering applications. Up to now, the vast majority of train impingement studies have been applied with low frequency and low Weber numbers (We < 500) like in [5,6]. The preferred liquids are usually DI water [1,7] (especially for experiments at high temperatures), engineered liquids [8,9] (e.g., HFE-7100 thanks to their low boiling points), and ethanol [10,11]. Moreover, our research group has been working on the splashing, boiling, and the Leidenfrost effect in steady-state [12,13] and transient conditions [11,14,15].

In addition to the splashing, spreading, and Leidenfrost phenomena, thermal gradients are also in the scope of the droplet train impingement studies since the thermal-driven boundary layers and thermal gradients can give useful insights for a better understanding of evaporation behavior on the target surface. However, the number of thermal-related droplet train impingement studies are very few except for some significant works like [16,17], which performed experimental and numerical studies for defining thermal boundary layers around the droplet impact area. Thus, in this study, the main contribution is to investigate the thermal flow behaviors of the impinged droplets on the target surfaces using a thermographic camera. Secondly, unlike the majority of train impingement studies, we applied a droplet train with an incline of 63 degrees instead of vertical impingement. Hereby, we aim to observe the impact of inclined flow direction on the impact area. Also, to better mimic the real conditions, we created small temperature gradients on the target surface because it is a fact that target surfaces have generally temperature gradients whilst most of the train impingement studies have been applied to the uniform target temperature. Ethanol is preferred as a liquid due to its broad applications in various engineering processes. Aluminum and glass plates are used as target surfaces so that we can observe the impact of substrate thermal conductivity.

2 Experimental Setup

The experimental setup consists of a pressurized tank filled with ethanol liquid, ethanol flow measurement sensors (flow meter and pressure sensor), droplet nozzle for droplet train, piezoelectric ceramic element and function generator for generating droplets from the ethanol flow, copper holder (insulated) for heating the target substrate, cylindrical heating cartridge for heating power in the copper block, thermographic camera, laptop, and power supply unit. The schematic of the experimental setup is shown in Fig. 1. Ethanol was provided from Sigma-Aldrich with a purity of ≥99.9%; density of 789 kg/m^3; surface tension of 0.022 N/m; dynamic viscosity of 0.012 Pa·s; and boiling point of 78.4°C. The impingement temperature of ethanol is 26°C. The thermographic camera model is ImageIR® 8300 (Germany) with 640 × 512 resolution whereas the droplet generator system is from FMP Technology GmbH (Germany). Furthermore, as mentioned in the Introduction section, the substrate is

unsymmetrically placed onto the copper block to provide small temperature gradients on the surface before impinging the droplet.
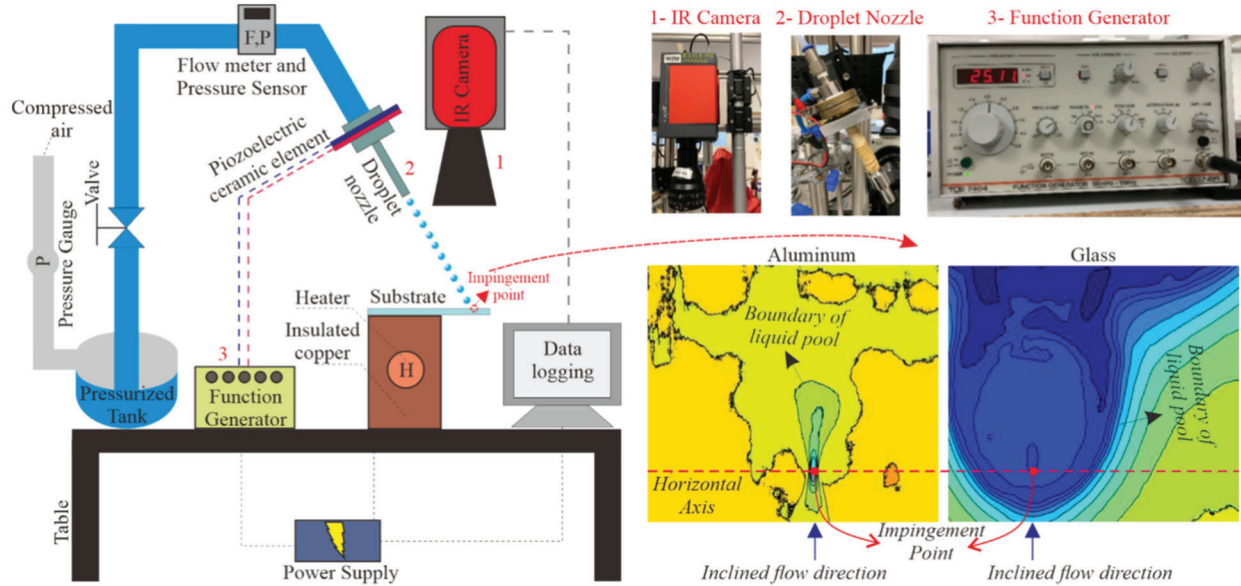

Figure 1: Simplified schematic of the ethanol droplet train impingement system with thermal images of aluminum and glass surfaces

Thermographic images of droplet train impingements on aluminum and glass surfaces are also shown for illustrative purposes in Fig. 1. To better clarify the impingement behaviors, a horizontal axis is drawn, and the flow dynamics are observed according to the top/bottom of the axis and the impingement point (first touch of the droplet). It must be noted that the free-curved black lines on the aluminum images are due to the reflection of aluminum surface, which negatively affects the thermographic camera measurement. That is, both lighter and darker yellow regions are dry (non-wetted) surfaces but color transition was observed due to the reflection of aluminum material. This concern is not valid for glass measurements because the black tape is applied to the bottom surface of the glass substrate while the thermographic camera collects temperature values from the top surface. To better illustrate, the boundaries of observed liquid pools are also shown in Fig. 1. For the temperature accuracy, both aluminum and glass temperature measurements via thermographic camera were calibrated via thermocouple measurements, which were collected from the substrates in parallel with the thermographic camera measurements. The calibration between the thermocouple and thermographic camera measurements was done in the MATLAB environment; then, the measured temperatures were plotted in the same tool. Furthermore, the physical characteristics of the generated droplets are defined with Weber number (We) and Reynolds number (Re) as presented below:

$$\mathrm{We} = (\rho \cdot v^2 \cdot \mathrm{d})/\sigma \tag{1}$$

$$\mathrm{Re} = (\rho \cdot v \cdot \mathrm{d})/\mu \tag{2}$$

where ρ is the density of the ethanol, v is the droplet velocity, d is the droplet diameter in the air, σ is the surface tension, and μ is the viscosity. According to the system calibration and measurements, Table 1 presents the droplet characteristics for droplet impingements to aluminum and glass substrates. It is seen that the We values are different between the two substrates due to variations in droplet spacing (l) and

frequency (f). However, the difference does not affect the hydrodynamic performance. The reason behind the observed difference is very small changes in the decimal places of the droplet spacing and the frequency values although both droplet diameter in air and the droplet nozzle diameter are the same whilst the supplied flow rate and the pressurized tank pressure are the same in both experiments as well. It is worth noting that the changes in the droplet in air, the droplet nozzle diameter and droplet velocity result in higher We differences, but they are the same in this study.

Table 1: Main characteristics of droplet impingement

Droplet parameters	Experiments on aluminum surface	Experiments on glass surface
D_0 (μm)	150	150
d (mm)	0.2	0.2
l (mm)	0.42	0.46
f (kHz)	25.1	25.5
We	792	998

3 Results and Discussion

The thermographic observation allows us to explain the droplet train impingement behaviors according to the droplet spreading area and liquid accumulation. The droplet spreading is based on the energy balance between the supplied ethanol liquid via droplet train and the liquid consumption via evaporation rate and/or droplet splashing. Therefore, in case of a high evaporation rate of a high splashing amount (via micro splashes or secondary splashing droplets), the spreading area becomes smaller. However, if the evaporation rate or the splashing amount is not enough, the spreading area becomes greater due to the insufficient amount of evaporation rate. Both evaporation rate and splashing phenomena can be explained as functions of the surface energy levels, which are simply based on the surface temperature and thermophysical characteristics of the substrate. Thermal conductivity is one of the most crucial characteristics of the surface. The surface energy level is higher for the substrates that have higher thermal conductivity values. Also, the increase of surface temperature improves the surface energy level. In fact, surface roughness is another parameter for defining the mechanistic background of the surface energy level; however, we neglect the impact of surface roughness in this study because both substrates (aluminum and glass) have small roughness values. To better explain the above-mentioned relations between surface temperature/surface characteristics and the surface energy level, Fig. 2 shows the thermographic measurement of the inclined ethanol droplet train impingement on the aluminum and glass surfaces at approximate surface temperature values of 140°C and 170°C.

Fig. 2 infers that the aluminum surface provides a faster evaporation rate than the glass surface thanks to its much higher thermal conductivity. The spreading area and the liquid accumulation region (see Fig. 1 for the definition of liquid accumulation region) are extremely smaller compared to the spreading area and liquid accumulation region of the glass surface. Thus, even though the supplied ethanol flow is nearly the same for both aluminum and glass surfaces, the aluminum surface achieves a higher evaporation rate. Moreover, when the impact of surface temperatures is compared, the increase of (approximately) 30°C shrinks the liquid accumulation region on the aluminum surface whereas the liquid accumulation region does not significantly change but the thermal gradient becomes smaller for the glass surface. According to the observed images, it can be said that the surface energy level of the glass is not enough to achieve the required evaporation rate at the surface temperatures of 140°C or 170°C; thus, higher surface temperatures are needed to shrink the liquid accumulation regions and increase the evaporation rate. For

the aluminum substrate, the surface energy level achieves a sufficient amount of evaporation rate and the accumulated liquid region becomes smaller. Fig. 3 illustrates the thermographic observation of aluminum and glass surfaces at higher surface temperature values up to the approximate value of 240°C.
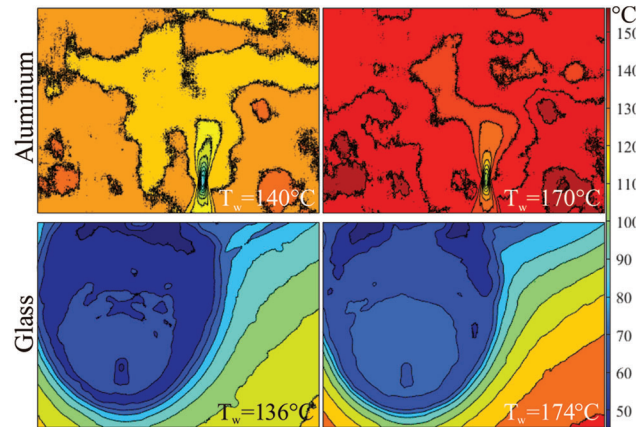

Figure 2: Thermographic images of the inclined ethanol droplet impingement on aluminum and glass surfaces at approximate surface temperature values of 140°C and 170°C
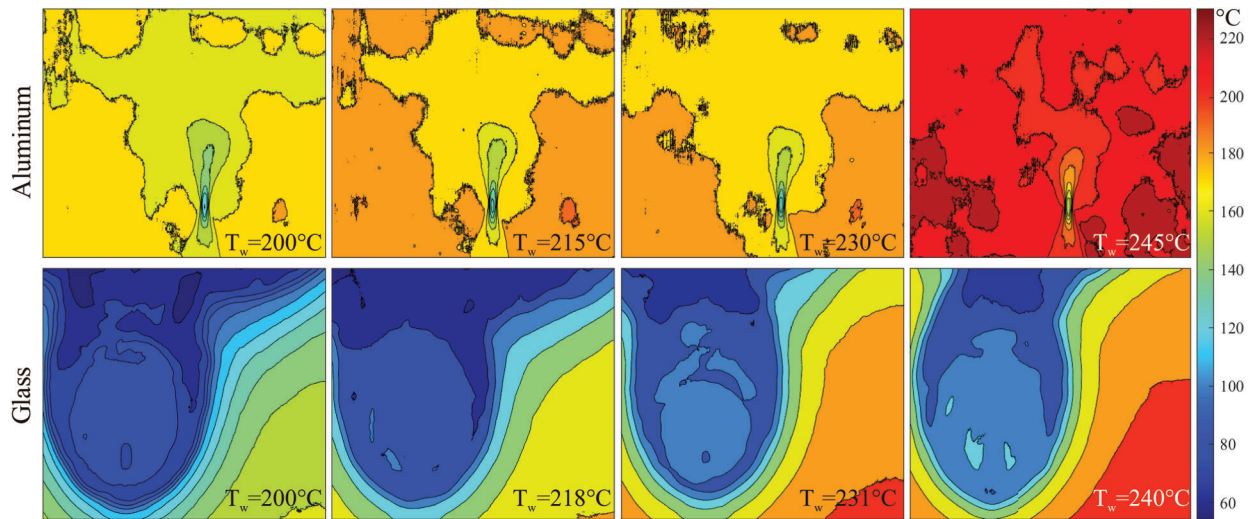

Figure 3: Thermographic images of the inclined ethanol droplet impingement on aluminum and glass surfaces at approximate surface temperature values from 200°C to 240°C

The results deduce that the increase of surface temperature dramatically improves the surface energy levels, which can be observed not only for aluminum but also for glass substrate. The liquid accumulation region on the aluminum surface significantly diminishes from 200°C to 240°C and the droplet impact area becomes like *a point heat sink*. On the other hand, the glass surface has still large accumulation pools at high surface temperature values, but it is clear that the liquid accumulation region becomes smaller by rising of the surface temperature. For example, at the surface temperature of 240°C, the liquid accumulation has the minimum area and the observed ethanol flow at the top of the image is mostly due to the inclined flow direction (see Fig. 1 for explanation). Furthermore, it is also seen that the increase of surface temperature changes the temperature gradient within the droplet impact area. Due to

the high thermal conductivity of aluminum, the temperature gradient dramatically decreases in the droplet impact area. For the glass surface, temperature gradients decrease like in the aluminum surface, but the decrement rate is not as high as in the aluminum.

Following the main outcomes of the observed thermal images, it can be said that the thermographic images are useful to detect the temperature gradients around the droplet impact area and on the surface. Using the temperature gradients, detailed quantitative calculations can be done via image processing techniques including the data driven-based algorithms. In addition, statistical heat transfer analysis can be done by locating thermocouples at different depths in the substrate; hereby, heat flux calculations can be performed by using the temperature difference between the surface and a certain depth value. However, it must be noted that the accuracy of the suggested applications directly depends on the quality of the collected thermal images; therefore, the calibration must be done well.

4 Conclusions

The presented study performed ethanol droplet train impingement on aluminum and glass surfaces with an incline of 63 degrees in the surface temperature ranges of 140°C–240°C. Boiling behaviors were observed via a thermographic camera with the resolution of 640×512, and the results were compared to one another according to the accumulated liquid pool and droplet impact area. In both glass and aluminum experiments, the generated droplet had the same diameter with 0.2 mm using the droplet pinhole diameter of 150 μm. Weber numbers were calculated as 792 and 998 for the aluminum and glass surfaces, respectively. The main conclusion of the study is presented as follows:

- Due to the higher thermal conductivity of aluminum, the droplet impact area and liquid accumulation region were dramatically smaller than the impact area and accumulation region on the glass surface.
- From 140°C to 240°C, aluminum had a sufficient surface energy level to keep the liquid accumulation region small, which were signs of a higher evaporation rate.
- The liquid accumulation region was large on the glass region at 140°C; however, it decreased by rising of the surface temperature. Nevertheless, even though the surface temperature increment improved the surface energy level, there were still accumulated ethanol liquid on the glass surface, which was due to the lower thermal conductivity performance of the glass.
- Temperature gradients in the impact area decreased by rising of the surface temperature. At high surface temperatures, the droplet impact area behaved like a *point heat sink* due to a very high evaporation rate. For the glass substrate, the liquid accumulation region shrank dramatically but it was not like a point heat sink; still like a circular region.

In light of the foregoing conclusions, future works can be suggested to improve the thermographic observation. At first, higher resolution thermal imaging can provide a more detailed investigation, especially in the droplet impact area. Also, in the case of using high-speed thermal imaging, the transient transitions of the impact area and liquid accumulation can be observed and detailed image-based measurement can be done for quantitative assessments. Furthermore, image processing-and data driven-based algorithms can be preferred to predict the thermal flow behavior on the substrate surface. In the case of collected video files via thermographic camera, the video input can be used to perform extrapolative transient predictions of thermal flow trends on the surface as previously proposed in references [18,19]. Last but not least, statistical and/or quantitative heat transfer calculations can be conducted locating thermocouples at various depths of the substrate; hereby, the temperature difference between the surface and the certain depths presents sufficient data for heat flux calculation. Since the current study was carried out for two different substrates, which were aluminum and glass, the above-mentioned future works can also be applied to other substrate types at different droplet diameters or Weber numbers.

Conflicts of Interest: The authors declare that they have no conflicts of interest to report regarding the present study.

References

1. Li, J., Zhang, H., Liu, Q. (2019). Dynamics of a successive train of monodispersed millimetric-sized droplets impact on solid surfaces at low Weber number. *Experimental Thermal and Fluid Science, 102,* 81–93. DOI 10.1016/j.expthermflusci.2018.08.029.

2. Fathi, S., Dickens, P. M., Hague, R. J. M., Khodabkhski, K., Gilbert, M. (2008). Analysis of droplet train/moving substrate interactions in ink-jetting processes. *2008 International Solid Freeform Fabrication Symposium,* pp. 230–238. Texas, USA.

3. Zhang, T., Tsai, H. M., Alvarado, J. (2014). Effects of single and double streams of droplet impingements on surface cooling. *Atomization and Sprays, 24,* 875–893. DOI 10.1615/AtomizSpr.2014007382.

4. Lee, J. B., Lee, S. H. (2011). Dynamic wetting and spreading characteristics of a liquid droplet impinging on hydrophobic textured surfaces. *Langmuir, 27,* 6565–6573. DOI 10.1021/la104829x.

5. Sellers, S. M., Black, W. Z. (2008). Boiling heat transfer rates for small precisely placed water droplets on a heated horizontal plate. *Journal of Heat Transfer, 130,* 054504. DOI 10.1115/1.2884183.

6. Gradeck, M., Seiler, N., Ruyer, P., Maillet, D. (2013). Heat transfer for Leidenfrost drops bouncing onto a hot surface. *Experimental Thermal and Fluid Science, 47,* 14–25. DOI 10.1016/j.expthermflusci.2012.10.023.

7. Dunand, P., Castanet, G., Gradeck, M., Lemoine, F., Maillet, D. (2013). Heat transfer of droplets impinging onto a wall above the Leidenfrost temperature. *Comptes Rendus Mécanique, 341,* 75–87. DOI 10.1016/j.crme.2012.11.006.

8. Zhang, T., Muthusamy, J. P., Alvarado, J. L., Kanjikarat, A., Sadr, R. (2016). Numerical and experimental investigations of crown propagation dynamics induced by droplet train impingement. *International Journal of Heat and Fluid Flow, 57,* 24–33. DOI 10.1016/j.ijheatfluidflow.2015.10.003.

9. Zhang, T., Alvarado, J. L., Muthusamy, J. P., Kanjikarat, A., Sadr, R. (2017). Heat transfer characteristics of double, triple and hexagonally-arranged droplet train impingement arrays. *International Journal of Heat and Mass Transfer, 110,* 562–575. DOI 10.1016/j.ijheatmasstransfer.2017.03.009.

10. Shen, S., Tong, W., Duan, F. (2020). Hydrodynamic pattern transition of droplet train imping onto heated titanium substrates with or without nanotube coating. *International Journal of Heat and Mass Transfer, 163,* 120409. DOI 10.1016/j.ijheatmasstransfer.2020.120409.

11. Kanbur, B. B., Hui, M. L. Z., Duan, F. (2020). Transient transition of high speed and high-frequency ethanol droplet train impingement on the heated indium tin oxide (ITO) surface. *5th International Conference on Smart and Sustainable Technologies (SpliTech),* pp. 1–6. Split, Crotia.

12. Qiu, L., Dubey, S., Choo, F. H., Duan, F. (2015). Splashing of high speed droplet train impinging on a hot surface. *Applied Physics Letters, 107,* 164102. DOI 10.1063/1.4934531.

13. Qiu, L., Dubey, S., Choo, F. H., Duan, F. (2019). High jump of impinged droplets before leidenfrost state. *Physical Review E, 99,* 033106. DOI 10.1103/PhysRevE.99.033106.

14. Qiu, L., Dubey, S., Choo, F. H., Duan, F. (2016). The transitions of time-independent spreading diameter and splashing angle when a droplet train impinging onto a hot surface. *RSC Advances, 6,* 13644–13652. DOI 10.1039/C5RA26314J.

15. Kanbur, B. B., Hui, M. L. Z., Duan, F. (2021). Transient hydrodynamic patterns of high Weber number ethanol droplet train impingement on heated glass substrate. *International Communications in Heat and Mass Transfer, 126,* 105451. DOI 10.1016/j.icheatmasstransfer.2021.105451.

16. Trujillo, M. F., Lewis, S. R. (2012). Thermal boundary layer analysis corresponding to droplet train impingement. *Physics of Fluids, 24,* 112102. DOI 10.1063/1.4766195.

17. Trujillo, M. F., Alvarado, J., Gehring, E., Soriano, G. S. (2011). Numerical simulations and experimental characterization of heat transfer from a periodic impingements of droplets. *Journal of Heat Transfer, 133,* 122201. DOI 10.1115/1.4004348.

18. Kanbur, B. B., Kumtepeli, V., Duan, F. (2020). Thermal performance prediction of the battery surface via dynamic mode decomposition. *Energy, 201,* 117642. DOI 10.1016/j.energy.2020.117642.

19. Tanis-Kanbur, M. B., Kumtepeli, V., Kanbur, B. B., Ren, J., Duan, F. (2021). Transient prediction of nanoparticle-laden droplet drying patterns through dynamic mode decomposition. *Langmuir, 37,* 2787–2799. DOI 10.1021/acs.langmuir.0c03546.